Polymer 50 (2009) 3196–3203

Contents lists available at ScienceDirect

Polymer

journal homepage: www.elsevier.com/locate/polymer

Sulfonated poly(ether ether ketone) membranes crosslinked with sulfonic acid containing benzoxazine monomer as proton exchange membranes

Yun-Sheng Ye [a], Ying-Chieh Yen [a], Chih-Chia Cheng [a], Wen-Yi Chen [b], Li-Tuan Tsai [b], Feng-Chih Chang [a,*]

[a] Institute of Applied Chemistry, National Chiao-Tung University, Hsin-Chu, Taiwan
[b] Material and Chemical Research Laboratories, Industrial Technology Research Institute, Chutung, Taiwan

ARTICLE INFO

Article history:
Received 12 November 2008
Received in revised form
27 April 2009
Accepted 29 April 2009
Available online 12 May 2009

Keywords:
Benzoxazine
Proton exchange membrane
SPEEK

ABSTRACT

The incorporation of benzoxazine (Ba) or sulfonic acid containing benzoxazine (SBa) as a crosslinking agent in SPEEK proton exchange membrane (PEM) can substantially improve the SPEEK membrane performance. The SPEEK–SBa membranes give higher effective selectivity than corresponding SPEEK–Ba membranes under close crosslinker loading and thus are more suitable to be used in direct methanol fuel cells. The best achieved SPEEK–SBa composition (SBa40) gives reasonable proton conductivity (0.91×10^{-2} S cm^{-1}) but significantly lower methanol permeability (6.5×10^{-8} S^2 cm^{-1}). The achieved effective selectivity (Φ = SPEEK–SBa40: 14.0×10^4 S s cm^{-3}) is substantially higher than the plain SPEEK ($\Phi = 7.24 \times 10^4$ S s cm^{-3}) which has great potential for practical applications in DMFCs.

1. Introduction

Proton exchange membrane (PEM) is key component of solid polymer electrolyte fuel cells (PEFCs) which provides an ionic pathways for proton transfer and prevents mixing of the reactant gases [1–5]. The perfluorosulfonic acid ionomer Nafion is one of the most studied materials for application as a solid polymer electrolyte membrane because of its chemical and physical stability at moderate temperatures and its high proton conductivity arising from its nanophase-separated morphology and highly interconnected ionic channels [6–9]. There are, however, several drawbacks which have seriously limited Nafion's further applications including, high cost, high methanol permeability, and environmental inadaptability with other materials [10–12]. Therefore, one of the most important challenges for current fuel cell research is the development of low-cost nonfluorinated membrane materials exhibiting high conductivity and high performance. Certain sulfonated aromatic polymers meet certain of these requirements, including sulfonated poly(aryl ether) (SPAE) [13–18], sulfonated polyphosphazene (SPOP) [19], poly(benzimidazole) (PBI) [20–22], sulfonated polyimide (SPI) [23–26], and sulfonated poly(ether ether ketone) (SPEEK) [27,28]. To achieve sufficient proton conductivity, these sulfonated aromatic polymer membranes require a high degree of sulfonation, which, unfortunately, usually results in a high degree of water swelling and loss of their mechanical properties, making them impractical for use in fuel cell applications.

To overcome these problems, crosslinking appears to be an efficient and simple approach toward retarding the degree of methanol diffusion and water uptake, while enhancing the mechanical properties and dimensional stability. Many reports have described that the crosslinking of polymer electrolyte membranes [29–34] is able to significantly improve the chemical and mechanical stabilities, but tend to lower their proton conductivity. Thus, the development of more efficient membranes with improved chemical and mechanical stabilities without detrimentally affecting the proton conductivity and methanol crossover remains an important challenge.

Polybenzoxazines possess good thermal, mechanical, and electronic properties and excellent dimensional stability [35–40]. Recently, benzoxazine monomers containing a variety of organic functional groups have been synthesized as precursors to form a new class of high performance polymers [41,42]. In this study, our aim was to synthesize a novel benzoxazine derivative (SBa) that contains sulfonic acid groups to serve as a crosslinker and also a bridge for ionic clusters in SPEEK membrane. This membrane is expected to improve the mechanical properties, dimensional stability, and the methanol crossover, in addition to improve the water sorption capability and the proton conductivity relative to other systems employing a crosslinker without sulfonic acid group.

* Corresponding author. Tel./fax: +886 3 5131512.
E-mail address: changfc@mail.nctu.edu.tw (F.-C. Chang).

0032-3861/$ – see front matter © 2009 Elsevier Ltd. All rights reserved.
doi:10.1016/j.polymer.2009.04.072

2. Experimental part

2.1. Materials

Victrex[R] PEEK grade 450G was purchased from Victrex. Aniline was obtained from Aldrich and used as received. 4-Aminobenzoic acid, hydroquinone, dicyclohexylcarbodiimide (DCC), and dimethylaminopyridine (DMAP) were purchased from Acros and used as received. Paraformaldehyde was obtained from Lancaster (US) and used as received. 4-Hydroxybenzenesulfonic acid salt was purchased from TCI (Tokyo, Japan) and used as received.

2.2. Hydroquinone/aniline-based benzoxazine (Ba)

A solution of hydroquinone (8 mmol), aniline (16 mmol), and paraformaldehyde (32 mmol) in 1,4-dioxane was heated under reflux for 3 days. After cooling, the mixture was washed with 1 N $NaOH_{(aq)}$ and then with distilled water (2×1 L). The 1,4-dioxane solution was dried (Na_2SO_4) and evaporated under vacuum to afford Ba as a yellow product (67% yield).

2.3. Hydroquinone/4-aminobenzoic acid-based benzoxazine (ABa)

A solution of hydroquinone (10 mmol), aminobenzoic acid (19.2 mmol), and paraformaldehyde (40 mmol) in 1,4-dioxane was heated under reflux for 3 days. After cooling to room temperature, the solvent was evaporated under reduced pressure. Ethyl ether was added while subjecting the oily residue to magnetic stirring, forming a white solid that was filtered and dried under reduced pressure (47% yield) [43].

HRMS (EI): m/z 431 [M^+]. E_{LEM}. A_{NAL}: cacld (%) for $C_{24}H_{20}N_2O_6$: C, 65.28; H, 8.08; N, 21.95. Found: C, 64.72; H, 7.88; N, 21.14.

2.4. Sulfonated benzoxazine (SBa)

DCC (12 mmol) and DMAP (1 mmol) were added to a solution of ABa (10 mmol) and 4-hydroxybenzenesulfonic acid salt (12 mmol) in dimethyl sulfoxide (25 mL) under a nitrogen atmosphere and then the reaction mixture was stirred for 24 h at 30 °C [44]. After cooling at room temperature, ethyl ether was added at 25 °C while subjecting the oil to magnetic stirring, a yellow precipitate was formed, which was filtered and recrystallized from a minimum amount of methanol while cooling in a refrigerator. The resulting white powder was filtered off and dried in a vacuum oven for 24 h (42% yield) (Scheme 1).

HRMS (EI): m/z 788 [M^+]. E_{LEM}. A_{NAL}: cacld (%) for $C_{36}H_{26}Na_2O_{12}S_2$: C, 54.82; H, 3.32; N, 3.55. Found: C, 55.85; H, 3.55; N, 3.68.

2.5. Sulfonation of PEEK

PEEK pellets (18 g) were added slowly to concentrated sulfuric acid (95–98 wt%, 500 mL) at room temperature under an argon atmosphere. After the PEEK had dissolved completely, the reaction mixture was stirred vigorously for 3 h at 55 °C [45]. After cooling at room temperature, the sulfonated PEEK (SPEEK) was recovered through precipitation into a large excess of ice water. The precipitated SPEEK was washed with distilled water until the pH was neutral and then dried, first at room temperature for 2 days and then in a vacuum oven at 80 °C for 24 h. A portion of this product (ca. 5 g) was neutralized in 1 M aqueous sodium hydroxide (500 mL) for 3 days to form the sodium salt SPEEK-Na. (32% yield).

The degree of sulfonation (DS) of SPEEK was determined to be 71.8% through ^{1}H NMR spectroscopic analysis in DMSO-d_6 solution [45].

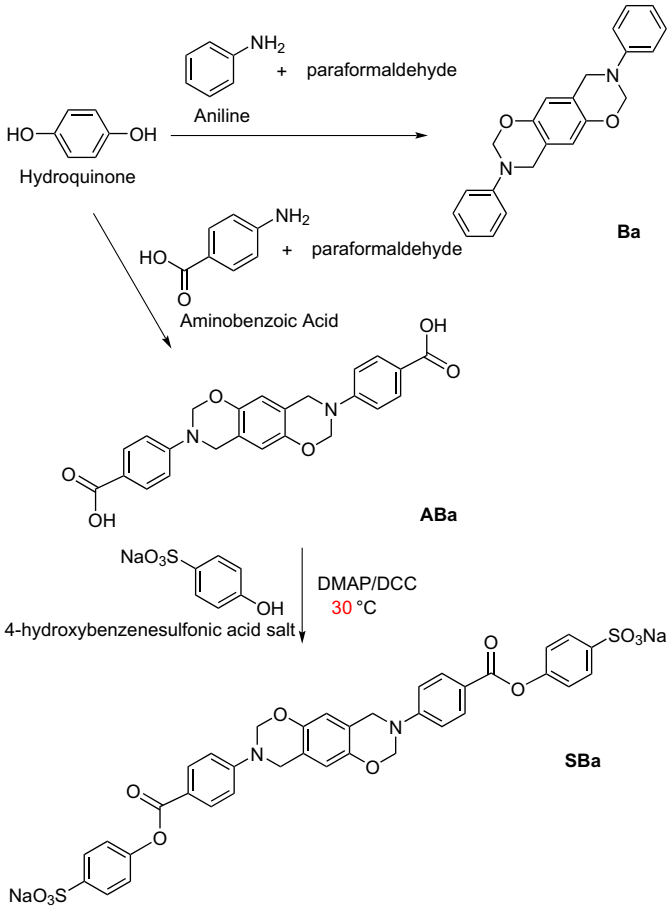

Scheme 1. Synthesis and chemical structures of the Ba and SBa.

2.6. Preparation of composite membranes

The SPEEK and SPEEK–benzoxazine (Ba, ABa, and SBa) composite membranes were prepared through solution-casting and evaporation. The SPEEK was dissolved in DMSO at room temperature as a 15 wt% solution. The various phr (5–50 phr) of Ba or SBa monomer (parts per hundreds of SPEEK matrix) was added to the polymer solution and the mixture stirred for ca. 6 h before casting onto a glass plate. The cast membrane was dried at 80 °C for 4 h, and then heated at 180 °C for 3 h to complete the crosslinking. Each membrane was soaked in methanol at room temperature to remove any residual solvent, and then it was peeled from the glass plate upon immersion in deionized water. The membranes were obtained in acidic form by immersing them into 1 M HCl solution for 24 h and then washing with deionized water until the pH reached in the range 6–7. The membrane in acid form was obtained with 100–150 μm in thickness.

2.7. Membrane characterizations

FTIR spectra were recorded in the range 4000–400 cm^{-1} using a Nicolet Avatar 320 FTIR spectrophotometer operated at a resolution of 1.0 cm^{-1} under a continuous flow of nitrogen. ^{1}H NMR spectra were recorded at 25 °C using an INOVA 500 MHz NMR spectrometer (^{1}H NMR spectroscopic analysis in DMSO-d_6 solution). The thermal degradation behavior of the membrane was measured using a Q100 thermogravimetric analyzer (TGA) operated from room temperature to 800 °C at a heating rate of

20 °C min^{-1} under a nitrogen atmosphere. The membrane morphologies were characterized using a JEOL JEM-1200CX-II transmission electron microscope (TEM) operated at 120 kV. To stain the hydrophilic domains, the membrane was converted into its Pb^{2+} form by immersing in 1 N $Pb(AC)_2$ (Lead acetate) solution overnight and then rinsing with water. The membrane was dried under vacuum at 80 °C for 12 h and then the sample was sectioned into 50-nm slices using an ultramicrotome. The slices were picked up with 200-mesh copper grids for TEM observation.

The completely dry SPEEK and Ba- and SBa-crosslinked SPEEK membranes were immersed in deionized water at room temperature for 24 h and then they were removed quickly, blotted with filter paper to remove any excess water from the membrane surfaces, and immediately weighed to obtain their wet masses (W_s). These membranes were then dried at 120 °C for 24 h before their dry weights (W_d) were measured. The water uptake (WU; %) was calculated using the following equation:

$$\mathrm{WU}(\%) = \frac{W_{wet} - W_{dry}}{W_{dry}} \times 100\% \quad (1)$$

The number of water molecules per ionic group, λ, was determined using the following equation:

$$\lambda = \frac{WU}{18 \times IEC} \quad (2)$$

The amount of free water in the fully hydrated membranes was determined using a DuPont TA2010 differential scanning calorimeter. The samples were first cooled from 25 to −60 °C and then they were heated to 50 °C at a rate of 5 °C min^{-1}. The mass of free water in the membrane was measured by integrating the area under the cooling curve and comparing it to the measured enthalpy of fusion for water (314 J g^{-1}).

The ion exchange capacities (IECs) were determined through titration with NaOH of the acid released from the protonic form of the membrane in 1 M NaCl. The ionic concentration was calculated using the following equation [29,46]:

$$[H^+] = \frac{IEC \times W_d / V_W}{1000} \quad (3)$$

where *IEC* refers to the titrated *IEC*, W_d is the weight of the dry membrane, and V_w is the volume of the wet membrane.

The proton conductivity of the membrane was measured using an ac electrochemical impedance analyzer (PGSTAT 30), where the ac frequency was scanned from 100 kHz to 10 Hz at a voltage amplitude of 10 mV. The membrane (1 cm in diameter) was sandwiched between two smooth stainless steel disk electrodes in a cylindrical Teflon holder. Measurement was taken after equilibrated for 30 min at 95% relative humidity (RH) and 30 °C. The proton mobility, μ, was estimated using the following equation [46,47]:

$$\mu = \frac{\sigma}{F[H^+]} \quad (4)$$

where F is Faraday's constant, σ is the proton conductivity of the membrane, and [H^+] is the concentration of protons.

Water desorption measurement was performed using a TGA Q100 to determine the weight change of the sample over time at 80 °C. The water diffusion coefficient was calculated using the following equation [48]:

$$\frac{M_t}{M_\infty} = 4\left(\frac{D_t}{\pi L^2}\right)^{1/2} \quad (5)$$

where D is the water diffusion coefficient, M_t/M_∞ represents the water desorption, and L is the membrane thickness.

The methanol diffusion coefficient across the membrane was measured using a two-chamber liquid permeability cell that has been described in detail previously [23–26]. One 50-mL chamber contained 5 M methanol solution and the other 50-mL chamber

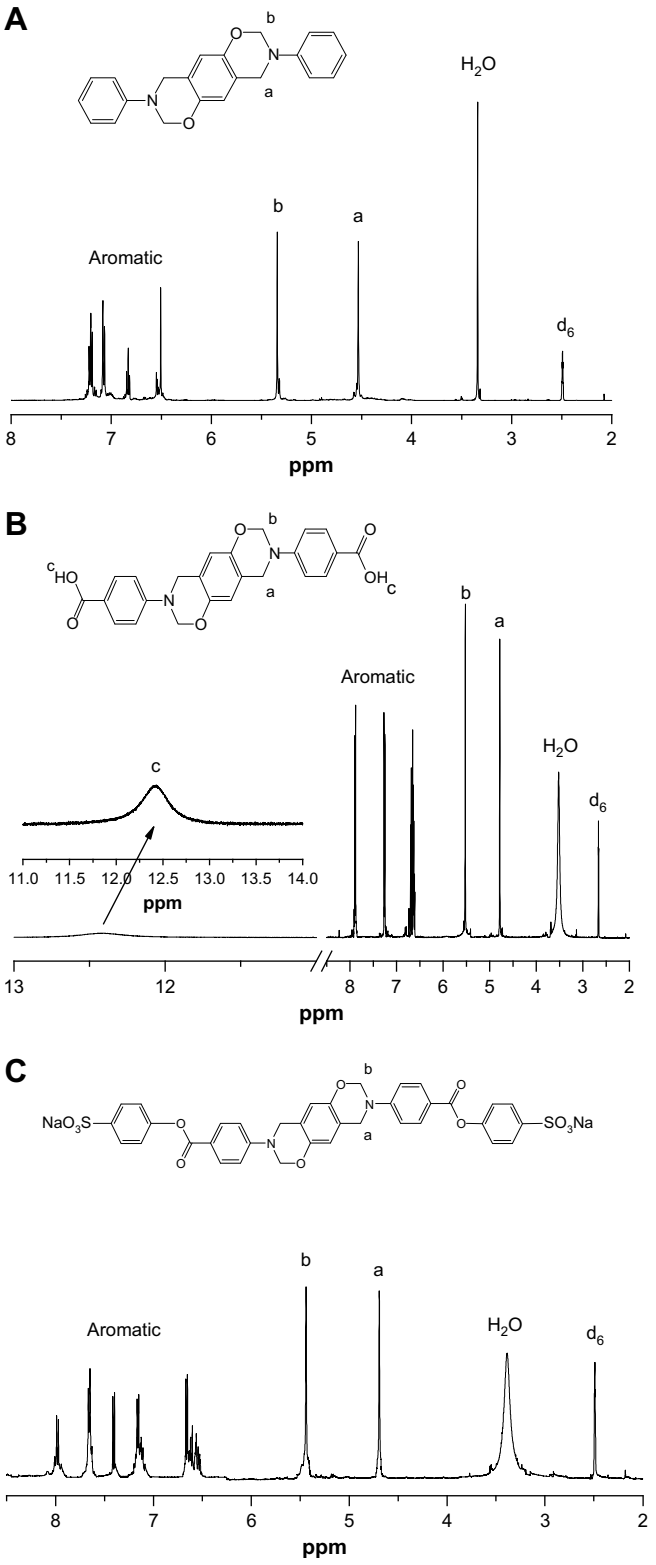

Fig. 1. The ^{1}H NMR spectrum of (A) Ba, (B) ABa and (C) SBa.

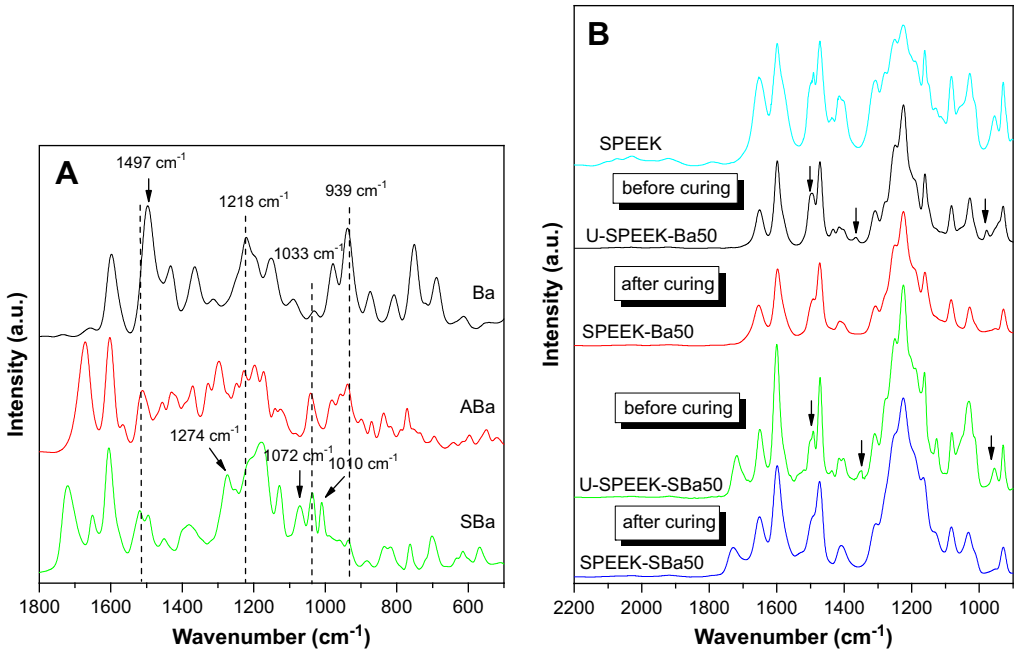

Fig. 2. The FTIR spectrum of (A) Ba, ABa and SBa (B) uncrosslinked (U-SPEEK–Ba50 and U-SPEEK–SBa50) and crosslinked (SPEEK–Ba50 and SPEEK–SBa50) membranes.

was filled with deionized water. The methanol concentrations in the water cell were determined periodically using a GC-8A gas chromatograph (SHTMADU, Tokyo, Japan). The methanol permeability was calculated using the following equation:

$$C_B(t) = \frac{A}{V_B}\frac{P}{L}C_A(t - t_0) \quad (6)$$

where L is the membrane thickness, A is the membrane area, C_A and C_B are the methanol concentrations in the methanol and water chambers, respectively, and P is the methanol diffusion coefficient.

3. Results and discussion

3.1. Preparations of Ba, ABa, and SBa

The chemical structures of Ba, ABa, and SBa (Scheme 1) were confirmed using FTIR and ^{1}H NMR spectroscopies. The ^{1}H NMR spectrum in Fig. 1(A) confirms the structure of Ba. The characteristic protons of the oxazine ring at 4.52 and 5.35 ppm are assigned to –Ar–CH_2–N– and –O–CH_2–N–, respectively. These aromatic protons appear as a multiplet at 6.5–7.2 ppm. Similarly, the ^{1}H NMR spectra of ABa and SBa [Fig. 1(B) and (C)] display the characteristic protons of their respective oxazine rings at 4.78 and 5.53 ppm.

The FTIR spectra of Ba, ABa, and SBa [Fig. 2(A)] display characteristic absorptions centered at 1220–1226 (asymmetric C–O–C stretching), 1030–1038 (symmetric C–O–C stretching), 920–950 and 1495–1518 cm^{-1} (vibrations of tetrasubstituted benzene ring). Characteristic absorption band assigned to their carboxyl groups appears at 1672 cm^{-1} (C=O stretching). Additionally, signals for the sulfonic acid groups of SBa are at 1274, 1072, and 1010 cm^{-1} (asymmetric and symmetric O=S=O vibrations) which are absent in the IR spectra of Ba and ABa.

3.2. Characterizations of Ba- and SBa-crosslinked membranes

SPEEK–Ba and SPEEK–SBa formed homogeneous and transparent solutions in DMSO prior to thermal curing. In our previous studies [49,50], we observed that the characteristic absorptions of these functionalized benzoxazines disappeared completely in their FTIR spectra after curing at 180 °C for 4 h or 210 °C for 1 h. Thus, we cured these SPEEK–Ba and SPEEK–SBa membranes at 180 °C for 4 h to thermally activate their crosslinking reactions. Fig. 2(B) indicates that the characteristic absorptions of the sulfonic acid groups of SPEEK appear at 1274, 1079, and 1023 cm^{-1} (asymmetric and symmetric O=S=O vibrations). After performing the curing cycle, the characteristic absorption bands at 954–976, 1358–1367 (tetra-substituted benzene ring) and 1501–1490 (CH_2 wagging) cm^{-1} of the SPEEK–Ba50 and SPEEK–SBa50 membranes disappeared completely, indicating that these blends were completely cured.

3.3. Membrane thermal stability

Fig. 3(A) and (B) presents the thermal stabilities of pure SPEEK, Ba- and SBa-crosslinked SPEEK membranes. The first weight loss,

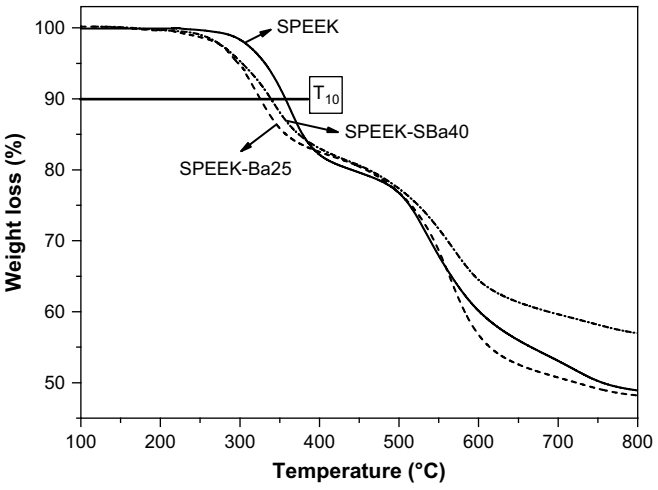

Fig. 3. TGA curves of SPEEK, SPEEK–Ba25 and SPEEK–SBa40.

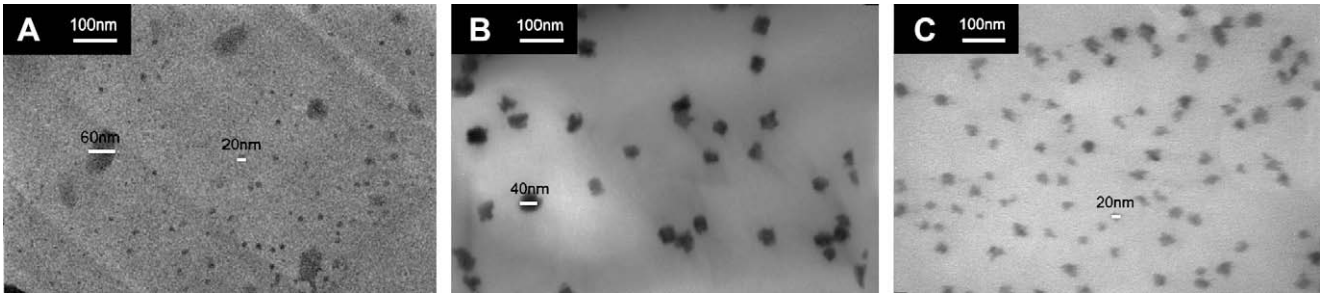

Fig. 4. TEM micrographs of the (A) SPEEK, (B) SPEEK–Ba, and (C) SPEEK–SBa membranes.

between 200 and 400 °C, is closely correlated to the thermal degradation of the sulfonic acid group or the main-chain polybenzoxazine. The second weight loss at temperatures above 400 °C is attributed to the thermal decomposition of the main chains of SPEEK and polybenzoxazine, [41,42] indicating that the thermal properties of these crosslinked PEMs are suitable for use in fuel cell applications. In this study, these properties of SPEEK–Ba25 and SPEEK–SBa40 were compared because they possess close crosslinker loading in terms of mole percent in SPEEK polymer matrix (SPEEK–Ba25: 21.0 mol%; SPEEK–SBa40: 17.2 mol%). The $T_{10\%}$ (the temperature of 10% weight loss) is higher than those of SPEEK–Ba25 implying that the physical crosslinking arises from specific interactions between sulfonic acid groups of SBa and SPEEK chains [51]. The crosslinker containing sulfonic acid groups (SBa) possesses stronger specific associations than the crosslinker without sulfonic acid groups (Ba) and results in higher thermal properties.

3.4. Membrane morphologies

The electrochemical properties of PEMs are closely related to their microstructure, especially the spatial distribution of their ionic sites [27,51–54]. The three images in Fig. 4 present the TEM micrographs of (A) SPEEK, (B) SPEEK–Ba, and (C) SPEEK–SBa membranes where the darker regions represent localized hydrophilic ionic clusters while the lighter parts represented hydrophobic moieties. The pure SPEEK membrane possesses non-uniform ionic clusters from a few nm up to 100 nm. The sizes of SPEEK–Ba25 domains [Fig. 4(B)] are mostly in the range between 40 and 50 nm. The size domains of SPEEK–SBa40 [Fig. 4(C)] are mostly in the range between 20 and 30 nm. The added Ba causes slight aggregation of the hydrophilic phase and results in overall larger ionic clusters but better distributed. The relatively better hydrophilic/hydrophobic distribution within the SPEEK–SBa40 [Fig. 4(C)] than SPEEK–Ba25 can be attributed to the existence of specific interactions between sulfonic acid groups of SBa and the SPEEK chains which can prevent the hydrophilic sulfonic groups of the pure SPEEK from aggregating into larger ionic clusters and lead to a random distribution of ion channels with good connectivity. The small ionic channels in the SPEEK–SBa40 membrane are more favorable for water absorption and proton transport as previously reported [33]. Scheme 2 illustrates the proposed proton transport and methanol permeability pathways of the SPEEK, SPEEK–Ba, and SPEEK–SBa membranes. The crosslinker with sulfonic acid groups (SBa) serves as separators to prevent ionic clusters aggregation. Moreover, these sulfonic acid groups of SBa could play a role as bridge between neighboring water-swollen pores, which could offer additional hydrophilic channels and facilitate proton transfer.

3.5. Ionic exchange capacity (IEC) and water behaviors

Table 1 lists the water uptake and IEC values of SPEEK, SPEEK–Ba, and SPEEK–SBa membranes. IEC values of SPEEK–Ba and –SBa membranes decrease with the increase of the crosslinker content due to lower content of sulfonic acid content. However, the IEC values of the SPEEK–SBa membranes are relatively higher than corresponding SPEEK–Ba membranes because of the additional sulfonic acid groups from the SBa.

Fig. 5 displays (A) the water uptake and (B) the λ values (water molecules per ionic group) of the SPEEK–Ba and –SBa membranes.

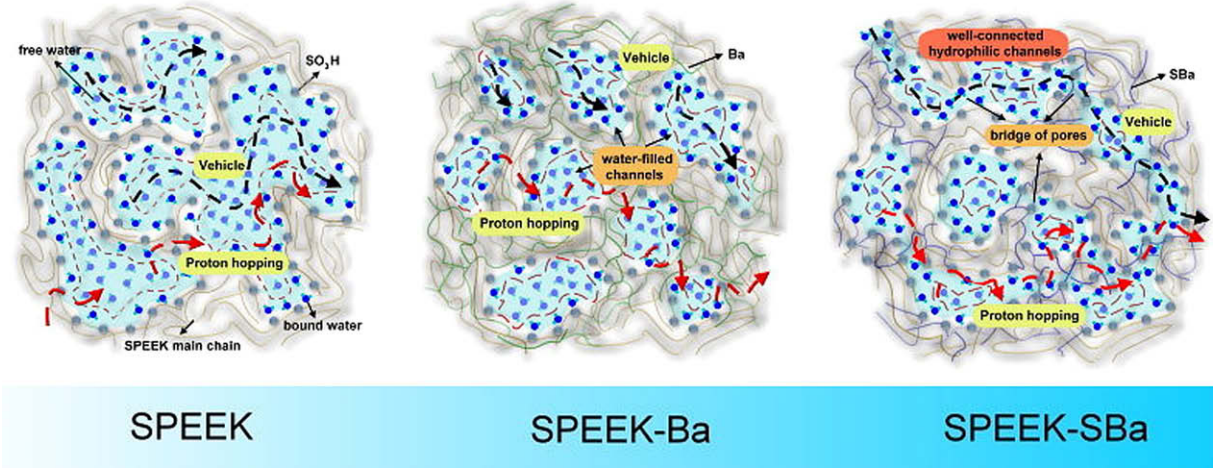

Scheme 2. Illustration on the state of water in the membranes and the proton transport mechanism in the membranes.

Table 1
IEC, water content, bound water ratio and water diffusion coefficient for desorptions of SPEEK, SPEEK–Ba and SPEEK–SBa membranes.

Sample	IEC (meq/g)	Water content (%)[a]	Bound water ratio [bound]/[total][b]	Water diffusion coefficient for desorptions × 10^5 ($cm^2\ s^{-1}$)
SPEEK	1.99	34.66	46.1	7.32
Ba5	1.85	27.21	51.3	5.9
Ba15	1.67	24.96	54.7	4.22
Ba25	1.45	22.22	57.4	2.89
Ba40	1.20	18.17	67.2	2.25
Ba50	0.97	15.02	73.5	1.29
SBa5	2.05	31.19	48.2	8.65
SBa15	1.93	30.57	52.6	7.44
SBa25	1.78	29.2	57.8	6.02
SBa40	1.62	26.69	65.1	4.56
SBa50	1.52	25.28	69.4	3.72

[a] Measured after immersion in water.
[b] Obtained using DSC.

The water uptake decreases upon increasing the Ba or SBa content in the SPEEK membrane because the free volume of the SPEEK matrix is restricted by crosslinking structure. Similar result has also been reported [29–34]. The SPEEK–SBa40 membrane exhibits higher water uptake relative than the SPEEK–Ba25 membrane, indicating that the incorporation of crosslinker with sulfonic acid groups tends to provide additional hydrophilic domains and results in enhanced water sorption capability as previously reported [33]. The effect of the SBa content on the water behavior of these crosslinked SPEEK membranes is shown in Fig. 5(B), the λ value increases slightly or remains nearly constant with the increase of the SBa content. The relatively higher λ values of the SPEEK–SBa membranes imply that the presence of additional sulfonic acid groups of SBa plays a role as a bridge between neighboring water-swollen pores to accommodate more water molecules from the additional hydrophilic channels as illustrated in Scheme 2 and TEM micrographs.

As listed in Table 1, for both SPEEK–Ba and –SBa membranes, the bound water ratio increased upon increasing the Ba and SBa contents. The size of hydrophilic domains decreases in the presence of a crosslinking structure. The water clusters at centers of hydrophilic domains come into closer contact for those sulfonic acid groups, thus, these water molecules tend to localized in limited areas, and thus increase the bound water ratio [55,56]. However, the bound water ratio of SPEEK–SBa40 is higher than that of SPEEK–Ba25 under close crosslinkers loading. The higher bound water ratio of the SPEEK–SBa is probably due to shorter distance between its neighboring sulfonic acid groups and its smaller hydrophilic domains as illustrated in Scheme 2 and Fig. 4(C).

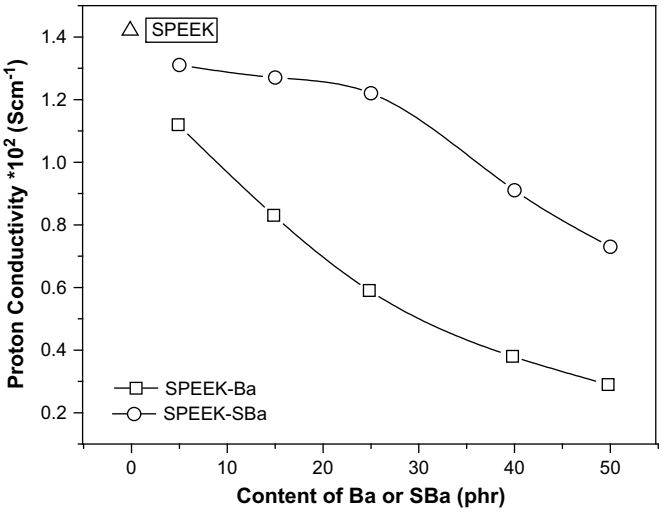

Fig. 6. Proton conductivity of the SPEEK, SPEEK–Ba and SPEEK–SBa membranes.

3.6. Proton conductivity

For crosslinked membranes, the type of crosslinker, the crosslinking density, and the microstructure all have dramatic effects on water uptake, state of water, and resultant proton conductivity [29–34]. Fig. 6 and Table 2 present the change in proton conductivity of

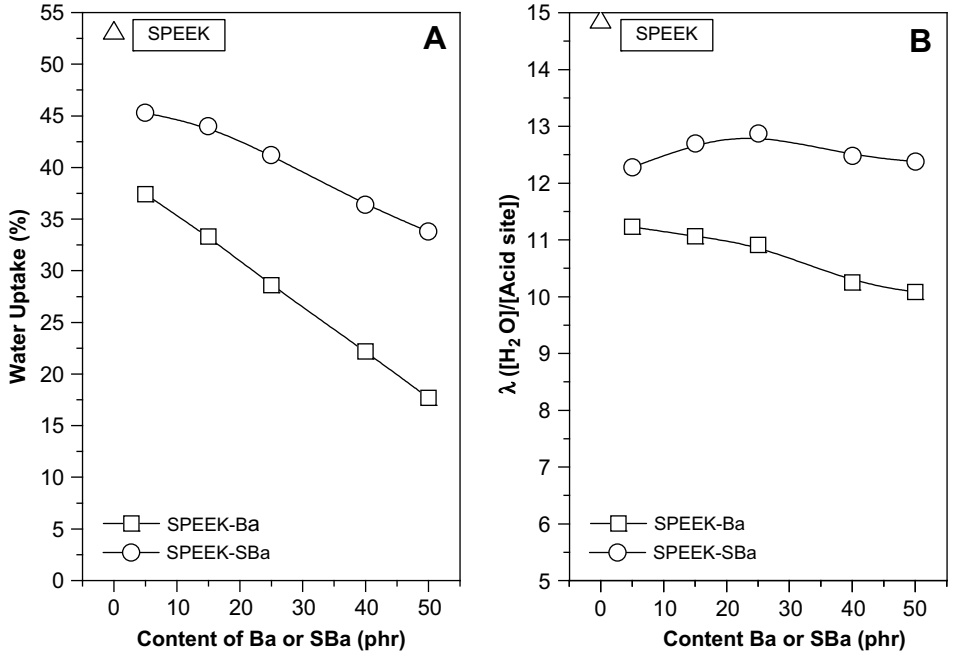

Fig. 5. (A) The water uptake and (B) The λ values (water molecules per ionic group) of SPEEK–Ba and SPEEK–SBa membranes.

Table 2
Proton conductivity, [H^+], proton mobility, methanol permeability and selectivity of SPEEK, SPEEK–Ba and SPEEK–SBa membranes.

Sample	Proton conductivity $\times 10^2$ (S cm^{-1})[a]	[H^+] (M)	Proton mobility $\times 10^4$ (cm^2 s^{-1} V^{-1})	Methanol permeability $\times 10^8$ (cm^2 s^{-1})	Selectivity $\times 10^4$ (S s cm^{-3})
SPEEK	1.42	1.29	1.141	19.6	7.24
Ba5	1.12	1.39	0.604	14.5	7.72
Ba15	0.83	1.43	0.411	10.2	8.13
Ba25	0.59	1.49	0.249	6.9	8.55
Ba40	0.38	1.58	0.186	4.3	8.83
Ba50	0.29	1.62	0.084	3.1	9.35
SBa5	1.31	1.33	1.021	16.3	8.04
SBa15	1.27	1.28	1.028	15.1	8.41
SBa25	1.22	1.25	1.012	11.4	10.7
SBa40	0.91	1.32	0.715	6.5	14.0
SBa50	0.73	1.40	0.540	5.1	14.31

[a] Proton conductivity measured at 30 °C and 95% relative humidity.

the SPEEK and Ba- and SBa-crosslinked SPEEK membranes as a function of the Ba and SBa content. The decreasing trend in the proton conductivity of the SPEEK–Ba membranes upon increasing the Ba content is similar to the water uptake as presented in Fig. 5(A). In contrast, the incorporation of SBa up to 25 phr results in only slight decrease in conductivity relative to pure SPEEK but shows dramatic decrease when the SBa content is higher than 25 phr. As described above, the incorporation of SBa-crosslinker results in higher water sorption capability to create additional hydrophilic channels mediated through sulfonic acid groups and results in higher proton conductivity than that of the Ba-crosslinked PEEK membrane. Similar result has been verified in proton mobilities of the crosslinked SPEEK membranes (Table 2). The water retention of membranes could provide indirect evidence of the proton conductive pathway. Generally, the larger size and well connection of transport channels will accelerate the water evaporation [27]. There is notable difference between Ba- and SBa-crosslinked SPEEK membranes. The diffusion coefficient of Ba-crosslinked SPEEK membrane significantly decreases with increase in the content of Ba in the SPEEK membrane. However, in the case of the SBa-crosslinked SPEEK membrane with low SBa content, the crosslinking led to an acceleration of the water evaporation regardless of the crosslinking effect on polymer chains. These results implied that these hydrophilic channels might be connected by additional SBa, and consequently the connection of hydrophilic channels will make the water in the membranes more

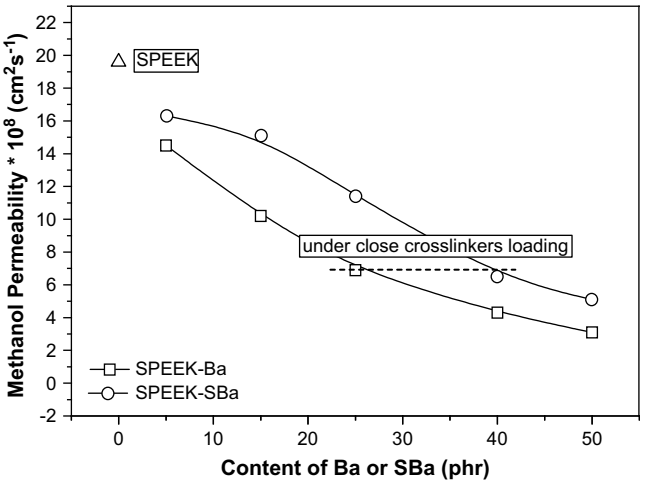

Fig. 7. Methanol permeability of the SPEEK, SPEEK–Ba and SPEEK–SBa membranes.

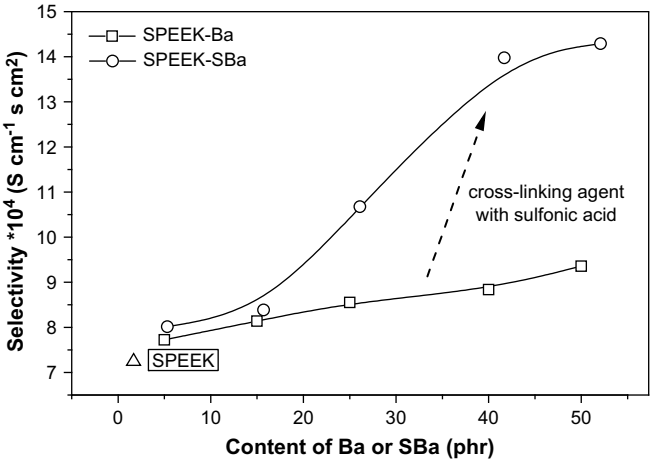

Fig. 8. Selectivity of the SPEEK, SPEEK–Ba and SPEEK–SBa membranes.

easily evaporate and the diffusion coefficient of water in membrane increase. On the contrary, the speed of diffusion of water decreased with the addition of Ba was attributed to poor-connected hydrophilic channels which will hinder the water diffusion of membranes. The results of water retention also proved that the crosslinking with SBa is more favorable to forming well-connected hydrophilic channels compared with the Ba.

3.7. Methanol permeability

Fig. 7 displays the methanol transport behavior of SPEEK, SPEEK–Ba, and SPEEK–SBa membranes, showing similar trend as water uptake [Fig. 5(A)] but slightly different on proton conductivity (Fig. 6). The presence of crosslinkings among those polymer chains prevents excessive water swelling and retards methanol crossover. Comparing the SPEEK–Ba25 and SPEEK–SBa40 membranes, the proton conductivity of the latter is almost twice of the former, but the methanol permeability of the SPEEK–SBa40 membrane is still higher than that of the SPEEK–Ba25 membrane (Fig. 7), representing that these sulfonic acid groups of SBa in the membrane fix the hydrophilic channels and attract mobile water molecules more effectively. According to above descriptions, increasing the bound water ratio (Table 1) and fixing the hydrophilic channels can reduce the methanol permeability of membranes effectively as previously reported [33,51,57].

The methanol permeability and the proton conductivity are the two major transport properties that determine fuel cell performance in DMFCs, lower methanol permeability and higher proton conductivity are both preferable. The ratio of the proton conductivity to the methanol permeability, Φ, is an effective parameter for evaluating the membrane performance in DMFCs. Fig. 8 displays the selectivity (Φ) against contents of PEEK–Ba25 and PEEK–SBa40, indicating that these benzoxazine crosslinkers are effective in improving the membrane performance in PEMs relative to SPEEK. Furthermore, SPEEK–SBa membranes exhibit higher Φ values as compared with the SPEEK and the SPEEK–Ba membranes because of their higher proton conductivity and lower methanol permeability of the SBa-crosslinked SPEEK membranes; thus, the SBa-crosslinker is more suitable to be used in direct methanol fuel cells.

4. Conclusions

For both SPEEK–Ba and SPEEK–SBa membranes, the water behavior, proton conductivity and methanol permeability behavior

are found to be governed by the dense network structure and lower cation-exchangable sites. However, the crosslinker with sulfonic acid groups (SBa) can provide well-connected hydrophilic channels as comparison of pristine SPEEK and SPEEK–Ba membranes. A decrease in proton conductivity relative to SPEEK is offset by considerable decrease in methanol permeability, thus resulting in overall higher effective selectivity (Φ). Comparing with effective selectivity between SPEEK–Ba and SPEEK–SBa, the SPEEK–SBa membranes give higher effective selectivity than SPEEK–Ba membranes under close crosslinker loadings and thus are more suitable to be used in direct methanol fuel cells. The best achieved SPEEK–SBa composition (SBa40) gives reasonable proton conductivity ($0.91 \times 10^{-2}\,S\,cm^{-1}$), significantly lower methanol permeability ($6.5 \times 10^{-8}\,S^2\,cm^{-1}$), and higher effective selectivity (Φ = SPEEK–SBa40: $14.0 \times 10^4\,S\,s\,cm^{-3}$) relative to the standard SPEEK ($\Phi = 7.24 \times 10^4\,S\,s\,cm^{-3}$).

References

[1] Appleby J, Foulkes RL. Fuel cell handbook. New York: Van Norstrand; 1989.
[2] Rikukawa M, Sanui K. Prog Polym Sci 2000;25:1463.
[3] Steele BCH, Heinzel A. Nature (London) 2001;414:345.
[4] Takimoto N, Wu L, Ohira A, Takeoka Y, Rikukawa M. Polymer 2009;50:534.
[5] Xie T, Hayden CA. Polymer 2007;48:5497.
[6] Mauritz KA, Moore RB. Chem Rev 2004;104:4535.
[7] Rollet AL, Diat O, Gebel G. J Phys Chem B 2002;106:3033.
[8] Gebel G, Atkins P. Polymer 2000;41:5829.
[9] James PJ, Elliott JA, McMaster TJ, Newton JM, Elliott AMS, Hanna S, et al. J Mater Sci 2000;35:5111.
[10] Hickner MA, Ghassemi H, Kim YS, Einsla BR, McGrath JE. Chem Rev 2004;104:4587.
[11] Roziere J, Jones DJ. Annu Rev Mater Res 2003;33:503.
[12] Liu BL, Robertson GP, Guiver MD, Shi ZQ, Navessin T, Holdcroft S. Macromol Rapid Commun 2006;27:1411.
[13] Gao Y, Robertson GP, Guiver MD, Mikhailenko SD, Li X, Kaliaguine S. Macromolecules 2005;38:3237.
[14] Roy A, Lee HS, McGrath JE. Polymer 2008;49:5037.
[15] Zhang F, Cui Z, Li N, Dai L, Zhang S. Polymer 2008;49:3272.
[16] Wang F, Hickner M, Ji Q, Harrison W, Mecham J, Zawodzinski TA, et al. Macromol Symp 2001;175:387.
[17] Bai Z, Houtz MD, Mirau PA, Dang TD. Polymer 2007;48:6598.
[18] Zhao C, Wang Z, Bi D, Lin H, Shao K, Fu T, et al. Polymer 2007;48:3090.
[19] Hofmann MA, Ambler CM, Maher AE, Chalkova E, Zhou XY, Lvov SN, et al. Macromolecules 2002;35:6490.
[20] Chuang SW, Hsu Steve LC. J Polym Sci Part A Polym Chem 2006;44:4508.
[21] Julien J, Régis M, Laurent G, Gérard G. Macromolecules 2007;40:983.
[22] Kumbharkar SC, Nazrul Islam Md, Potrekar RA, Kharul UK. Polymer, in press.
[23] Asano N, Aoki M, Suzuki S, Miyatake K, Uchida H, Watanabe M. J Am Chem Soc 2006;16:4465.
[24] Miyatake K, Watanabe M. J Mater Chem 2006;16:4465.
[25] Savard O, Peckham TJ, Yang Y, Holdcroft S. Polymer 2008;49:4949.
[26] Li N, Cui Z, Zhang Z, Xing Wei. Polymer 2007;48:7255.
[27] Li X, Zhang G, Xu D, Zhao C, Na H. J Power Sources 2007;165:701.
[28] Jones DJ, Rozière J. J Membr Sci 2001;185:41.
[29] Schmeisser J, Holdcroft S, Yu J, Ngo T, McLean G. Chem Mater 2005;17:387.
[30] Zhong S, Fu T, Dou Z, Zhao C, Na H. J Power Sources 2006;162:51.
[31] Zhong S, Cui X, Cai H, Fu T, Zhao C, Na H. J Power Sources 2007;164:65–72.
[32] Guo Q, Pintauro PN, Tang H, O'Connor S. J Membr Sci 1999;154:175.
[33] Lee CH, Part HB, Chung YS, Lee YM, Freeman BD. Macromolecules 2006; 39:755.
[34] Yin Y, Hayashi S, Yamada Q, Kita H, Okamoto KI. Macromol Rapid Commun 2005;26:696.
[35] Wang YX, Ishida H. Macromolecules 2000;33:8149.
[36] Chernykh A, Agag T, Ishida H. Polymer 2009;50:382.
[37] Allen DJ, Ishida H. Polymer 2008;49:613.
[38] Lin CH, Chang SL, Hsieh CW, Lee HH. Polymer 2007;48:7255.
[39] Allen DJ, Ishida H. Polymer 2007;48:6763.
[40] Laobuthee A, Chirachanchai S, Ishida H, Tashiro K. J Am Chem Soc 2001; 123:9947.
[41] Agag T, Takeichi T. Macromolecules 2001;34:7257.
[42] Agag T, Takeichi T. Macromolecules 2003;36:6010.
[43] Andreu R, Reina JA, Ronda JC. J Polym Sci Part A Polym Chem 2008;46:6091.
[44] Moore JS, Stupp SI. Macromolecules 1990;23:65.
[45] Huang RYM, Shao P, Burns CM, Feng X. J Appl Polym Sci 2001;82:2651.
[46] Siu A, Schmeisser J, Holdcroft S. J Phys Chem B 2006;110:6072.
[47] Saito M, Arimura N, Hayamizu K, Okada T. J Phys Chem B 2004;108:16064.
[48] Watari T, Wang HY, Kuwahara K, Tanaka K, Kita H, Okamoto K. J Membr Sci 2003;219:137.
[49] Wang CF, Su YC, Kuo SW, Huang CF, Sheen YC, Chang FC. Angew Chem Int Ed 2006;45:2248.
[50] Su YC, Kuo SW, Yei DR, Xu H, Chang FC. Polymer 2003;44:2187.
[51] Su YH, Liu YL, Sun YM, Lai JY, Wang DM, Gao Y, et al. J Membr Sci 2007; 296:21.
[52] Sauer BB, Mclean RS. Macromolecules 2000;33:7939.
[53] Ding JF, Chuy C, Holdcroft S. Adv Funct Mater 2002;12:389.
[54] Chen WF, Kuo PL. Macromolecules 2007;40:1987.
[55] Paddison SJ, Paul R. Phys Chem Chem Phys 2002;4:1158.
[56] Paddison SJ. Annu Rev Mater Res 2003;33:289.
[57] Park HB, Lee CH, Sohn JY, Lee YM, Freeman BD, Kim HJ. J Membr Sci 2006;285:432.